Torque-Speed Relationship of the Flagellar Rotary Motor of *Escherichia coli*

Xiaobing Chen and Howard C. Berg
Department of Molecular and Cellular Biology, Harvard University, Cambridge, Massachusetts 02138, and the Rowland Institute for Science, Cambridge, Massachusetts 02142 USA

ABSTRACT The output of a rotary motor is characterized by its torque and speed. We measured the torque-speed relationship of the flagellar rotary motor of *Escherichia coli* by a new method. Small latex spheres were attached to flagellar stubs on cells fixed to the surface of a glass slide. The angular speeds of the spheres were monitored in a weak optical trap by back-focal-plane interferometry in solutions containing different concentrations of the viscous agent Ficoll. Plots of relative torque (viscosity $\times$ speed) versus speed were obtained over a wide dynamic range (up to speeds of ~300 Hz) at three different temperatures, 22.7, 17.7, and 15.8°C. Results obtained earlier by electrorotation (Berg and Turner, 1993, *Biophys. J.* 65:2201–2216) were confirmed. The motor operates in two dynamic regimes. At 23°C, the torque is approximately constant up to a knee speed of nearly 200 Hz, and then it falls rapidly with speed to a zero-torque speed of ~350 Hz. In the low-speed regime, torque is insensitive to changes in temperature. In the high-speed regime, it decreases markedly at lower temperature. These results are consistent with models in which torque is generated by a powerstroke mechanism (Berry and Berg, 1999, *Biophys. J.* 76:580–587).

INTRODUCTION

The bacterial flagellar motor is a rotary engine embedded in the cell wall and cytoplasmic membrane; it is linked by the proximal hook to an external helical filament (reviewed by Macnab, 1996; Berry and Armitage, 1999). The motor is powered by protons (or in some species, sodium ions) driven inward across the cytoplasmic membrane. In *Escherichia coli*, the energy source is a protonmotive force, generated by respiration (for cells grown aerobically). The power input is protonmotive force $\times$ proton charge $\times$ proton flux. The power output is torque $\times$ angular velocity ($2\pi \times$ torque $\times$ rotational speed). Successful models for the motor mechanism must account for the observed dependence of torque on speed. These predictions can differ radically, for example, for ratchet mechanisms (in which the dissipation of proton free energy and motor rotation occur in different steps) and for powerstroke mechanisms (in which they occur in a single step). For ratchet mechanisms, torque drops rapidly with speed, and the torque-speed curve is concave upward; for powerstroke mechanisms, there can be a torque plateau, and the torque-speed curve is convex upward (Berry and Berg, 1999).

The torque-speed relationship for the flagellar motor of *E. coli* was measured earlier over a wide dynamic range by electrorotation (Berg and Turner, 1993). This was done by tethering a cell to glass by a single flagellar filament and applying torque to the cell body with a high-frequency rotating electric field (a technique pioneered by Washizu et al., 1993). When, at a given field intensity, the cell body is driven forward, it spins faster when the motor is intact (and thus is contributing to the effort) than it does when the motor has been broken (and is not). The torque contributed by the motor when it is intact is proportional to the difference in these two speeds. (One can break the motor by driving it backward.) However, the interpretation of these data is subject to simplifying assumptions, for example, that the torque due to internal friction in a broken motor is negligible compared to the torque due to the external viscous drag on the cell body. Also, there are artifacts due to ellipticity in the applied field that are important primarily when an intact motor is driven backward (Berry and Berg, 1999). Given these ambiguities, we sought to confirm the electrorotation results by independent means.

STRATEGY

The torque required to spin an inert object in a viscous medium is its rotational frictional drag coefficient times the angular velocity (see Berg, 1993, Chap. 6). For example, for a sphere of radius a rotating about a diameter in a medium of viscosity η, the frictional drag coefficient is $8\pi\eta a^3$. In a medium in which viscosity is independent of the rate of shear (a Newtonian medium), η is constant (independent of angular velocity). If the rotational geometry is fixed, the load line, the torque required to spin the object at a given speed plotted as a function of that speed, is straight, and its slope is proportional to η. Fig. 1 shows a hypothetical motor torque-speed relationship and two load lines, for the same object at two different viscosities. The motor will spin that object at the speed at which the torques balance, i.e., at the point of intersection of the torque-speed curve and the load line. Therefore, the torque-speed curve can be mapped by increasing the slope of the load line in a known way (by

Received for publication 9 August 1999 and in final form 19 October 1999.
Address reprint requests to Dr. Howard C. Berg, Department of Molecular and Cellular Biology, Harvard University, 16 Divinity Avenue, Cambridge, MA 02138. Tel.: 617-495-0924; Fax: 617-496-1114; E-mail: hberg@biosun.harvard.edu.

0006-3495/00/02/1036/06 $2.00

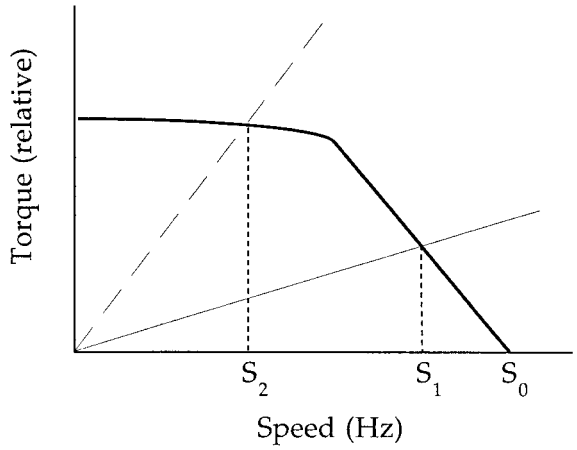

FIGURE 1 A hypothetical torque-speed curve for a flagellar motor (*thick line*) and two load lines (*thin lines*), one for a small sphere spinning in water (*solid line*) and the other for the same sphere spinning in a solution of Ficoll (*dashed line*). The motor will drive the sphere at the speeds indicated at the points of intersection of the thick and thin lines, i.e., at speeds S_1 and S_2, respectively. S_0 is the zero-torque speed.

increasing the viscosity of the external medium by a known amount) and by measuring the rotational speed. If one is to work over a wide dynamic range, the initial slope must be small, i.e., the object must be small. We accomplished this task by attaching small latex spheres to flagellar filament stubs and then changing the viscosity of the external medium by adding Ficoll. That the viscosities of solutions of Ficoll are well defined on this scale (and equal to the bulk viscosities) was confirmed by measurements of sedimentation rates of particles of similar size (diameter 0.3–0.4 μm).

MATERIALS AND METHODS

Chemicals, media, cells

Ficoll 400 (dialyzed and lyophilized) was from Sigma Chemical Co. (St. Louis, MO). Silica spheres (diameter 0.3 μm, density 1.96 g/cm^3, 10% solids) were from Bangs Laboratories (Fishers, IN). Polystyrene latex spheres (0.25 or 0.36 μm diameter, 2.6% solids) were from Polysciences (Warrington, PA). Tryptone was from Difco Laboratories (Detroit, MI). All other chemicals were reagent grade. Water was deionized (18 MΩ-cm) and filtered (0.2 μm). Motility medium was 10 mM KPO_4, 70 mM NaCl, 0.1 mM EDTA, 1 mM L-methionine, 0.05% (v/v) lactic acid (pH 7.0). Solutions of Ficoll (1–15% w/v) were made from a 40% (w/v) stock prepared in motility medium at room temperature, filtered through a cellulose-acetate membrane (0.22 μm), diluted with requisite volumes of motility medium, and stored frozen at −20°C. The bulk viscocities of these solutions were measured at the temperatures specified with a Cannon-Ubbelohde capillary viscometer (Cannon Instrument Co., State College, PA). Cells were *E. coli* strain KAF95 (Fahrner, 1995; see Berg and Turner, 1993). This strain rotates its motors exclusively counterclockwise (except at very low temperatures) and has a sticky filament phenotype. Cells were grown to midexponential phase in T-broth (1% tryptone, 0.5% NaCl) containing ampicillin (100 μg/ml; Sigma) and then washed into motility medium by repeated centrifugation at 3000 × *g*.

Sedimentation experiments

Silica beads were lyophilized and added to solutions of Ficoll at a final dilution of 1% solids. These mixtures were sonicated and transferred to Kimax melting-point capillary tubes (~1.2 mm i.d., 10 cm long; Kimble Scientific Products, Vineland, NJ). Mineral oil was added at either end of each tube to prevent evaporation, and the top ends were sealed with modeling clay. The tubes were mounted vertically in an aluminum block placed on top of a heat exchanger in a small vertical laminar flow hood (homemade), with the heat exchanger held at 22.7°C by a circulating water bath (Lauda RC 6; Brinkmann Instruments, Westbury, NY). The tubes were illuminated slantwise from behind and viewed from in front with a horizontal telescope equipped with an ocular cross hair and a vertical micrometer screw (Gaertner Scientific, Chicago, IL). A piece of black paper was put in back to enhance visual contrast. Sedimentation of the meniscus was followed for distances of a centimeter or more. When it became apparent that the silica particles sedimented more rapidly than expected, their diameters were measured by transmission electron microscopy and were found to be larger than advertised (0.45 ± 0.03 μm, $n = 75$).

Tethered bead experiments

Cells from a 10-ml culture were resuspended in 1 ml motility medium, and their flagellar filaments were sheared off by passing the suspension 50–80 times between two syringes equipped with 26-gauge needles and connected by a 6-cm length of polyethylene tubing (0.58 mm i.d.). The suspension was centrifuged (as before), and the cells were resuspended in 2–5 ml of motility medium. The cells were allowed to settle for 15 min onto the bottom window of a flow cell (Berg and Block, 1984). This window had been cleaned in ethanolic KOH and silanized with 4-aminobutyldimethyldimethoxysilane, as described in Berg and Turner (1993). Then unattached cells were washed away with motility medium, and a suspension of latex beads (~0.1% solids in motility medium) was added. After 2–5 min., unattached beads were washed away with motility medium. Rotation of the beads was followed by back-focal-plane interferometry in the optical trap described by Berry and Berg (1997), with the trap run at very low power (~2 mW at the trap focus). The cell, bead, and trap geometry is shown in Fig. 2. The *x* and *y* signals from the quadrant detector were low-pass filtered (8-pole Bessel, 250 Hz) and sampled (at 1024 or 2048 Hz) by a LabVIEW system (National Instruments, Austin, TX), as in Berry and Berg (1997). Rotational frequencies were determined from power spectra for successive 1-s blocks of data. Ficoll solutions were drawn into the flow cell manually via syringe. The volume required (typically 0.25 ml) to completely displace the previous solution was determined by monitoring motor speeds before, during, and after fluid exchange. The microscope objective (oil immersion) was thermostatted by a Peltier system similar to that described previously (Khan and Berg, 1983), and the temperatures in the flow cell at the point of observation were checked with a thermocouple thermometer (type T; Cole-Parmer, Vernon Hills, IL), using a junction

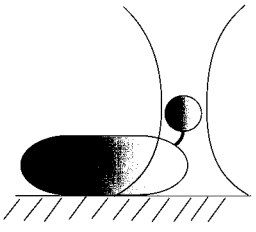

FIGURE 2 Rotation of a polystyrene latex bead (sphere) attached to a flagellar stub monitored in a weak optical trap, with the cell fixed to the surface of a glass coverslip.

made with 0.34-mm wires that was calibrated against a mercury thermometer traceable to the National Bureau of Standards. When the temperature setting was changed, 10–15 min was required for equilibration. When solutions were drawn into the flow cell set at temperatures below ambient, at least 1 min was allowed for equilibration.

RESULTS

Local and bulk viscosities

If Stokes' law is valid, the sedimentation rate of an isolated sphere of radius a and density ρ_s in a liquid of density ρ_l and viscosity η is $v = (2/9\eta)\ (\rho_s - \rho_l)ga^2$, where g is the acceleration due to gravity (see Berg, 1993, Eq. 4.21). This relationship has been found to be quite precise in water for spheres of the size used here (see Perrin, 1923, pp. 97–99). A dense ensemble of particles in a tube sediments more slowly than an isolated particle, so for the ensemble this equation needs to be multiplied by a factor that depends on particle size, average intraparticle distance, and tube size but not on viscosity (see Happel and Brenner, 1983, Chap. 8). For example, a suspension of silica particles that we used with 10% solids sedimented 60% as rapidly as one with 1% solids (Chen, 1999). At a fixed particle density (we used 1% solids) the sedimentation rate in a solution of Ficoll of density ρ_f and viscosity η_f relative to that in water at density ρ_w and viscosity η_w should be $v_f/v_w = (\eta_w/\eta_f)(\rho_s - \rho_f)/(\rho_s - \rho_w)$. Using water as a standard, we compared the sedimentation rates in different solutions of Ficoll relative to that in water and used this relationship to compute the local viscosity, η_f. We measured the bulk viscosity in a capillary viscometer. Fig. 3 compares the two. We conclude that Ficoll is a suitable viscous agent for use with particles on the 0.3–0.4-μm scale.

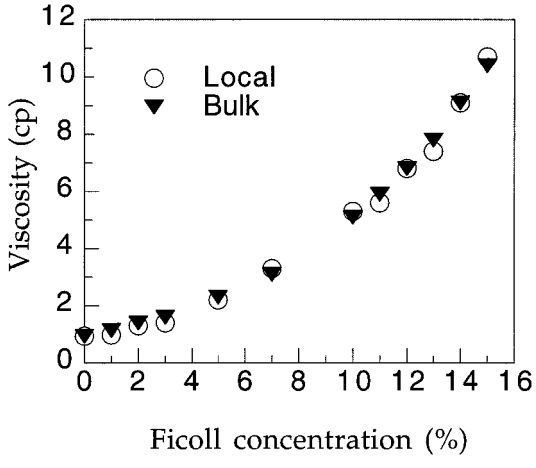

FIGURE 3 The local and bulk viscosities of solutions of Ficoll at 22.7°C. Standard deviations, obtained from linear fits to curves of sedimentation height versus time, were 1–3% of the mean.

Sensitivity of cells to light

It is known that the motility system can be damaged by intense blue light, e.g., when cells are observed by dark-field microscopy with a xenon arc (Macnab and Koshland, 1974). In preliminary experiments, we found that this is true even under phase contrast with a tungsten-halogen lamp (100-W Xenophot). The rotation speeds of cells tethered to glass by a single filament and illuminated in this way dropped significantly, beginning after 1 or 2 min and declining by a factor of 2 within ~10 min (Chen, 1999). This effect was eliminated by insertion of a 495-nm long-pass filter (e.g., GG495, 2 mm thick; Schott Glass Technologies, Durea, PA), after which rotation rates remained constant for periods of at least 15 min. Therefore, when cells were observed with visible light, e.g., while beads were being maneuvered into the optical trap, such a filter was always inserted between the halogen lamp and the microscope stage.

Motor torque-speed relationships

Fig. 4 *a* shows data collected from a single cell at 22.7°C over a period of 10 min, in which the contents of the flow

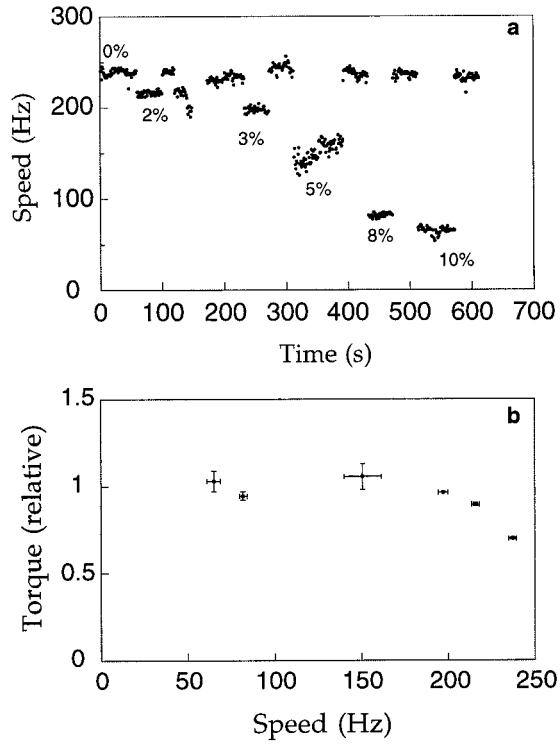

FIGURE 4 (*a*) Speeds measured during a bead-on-stub experiment at 22.7°C, shown as a function of time. When Ficoll was present, its concentration is indicated (% w/v; see Table 1). (*b*) The corresponding torque-speed plot. The error bars show standard deviations in the mean of the speeds measured for each set of points in *a*, with all of the data for speed in the motility medium combined into one set.

cell were shifted back and forth between motility medium and solutions of Ficoll in motility medium at five different concentrations. Fig. 4 *b* shows the corresponding torque-speed plot (viscosity × speed versus speed). Here the viscosity × speed data have been normalized by dividing by the mean of the viscosity × speed values near 60 Hz. The viscosities measured for the Ficoll solutions used in these experiments are shown in Table 1.

Fig. 5 shows cumulative data for cells at 22.7, 17.7, and 15.8°C. The linear regressions were made by an iterative procedure. In the first iteration, the data were divided into low-speed and high-speed sets by eye, and a linear regression was run for each. The point of intersection of the two lines was taken as a new boundary between the two data sets, and the regressions were repeated. The "knee speed," the point of intersection between the final regression lines, was substantially higher at higher temperatures (175 Hz at 22.7°C as compared to 83 Hz and 80 Hz at 17.7°C and 15.8°C, respectively). There are two dynamic regimes, one below the knee, in which relative torque is approximately constant (at 22.7°C, dropping from 1 to 0.92 between stall and 175 Hz), and another above the knee, in which the torque rapidly declines (at 22.7°C, dropping from 0.92 to 0 between 175 and 350 Hz). The "zero-torque speed" was deduced by extrapolation of the second regression line. At low speeds, torque is independent of temperature, as found earlier for tethered *Streptococcus* by Khan and Berg (1983). At high speeds, torque is strongly dependent on temperature. This is shown for data obtained with a single cell in Fig. 6, where the regression lines of Fig. 5 have been added to guide the eye. In motility medium, the speed dropped from ~180 to 110 Hz as the temperature was lowered. In 10% Ficoll, it remained near 40 Hz.

These results are consistent with those obtained earlier by electrorotation (Berg and Turner, 1993). In that work, the data were summarized in an idealized way (Berg and Turner, 1993, figure 16), with the assumption that the torque-speed curve was flat between stall and the knee. Here, instead of constructing curves from mean values for knee speeds and zero-torque speeds (as done earlier), we show the previous cumulative electrorotation data for all of the data points (Fig. 7). Figs. 5 and 7 are similar. The results obtained from the linear regressions are compared in Table 2.

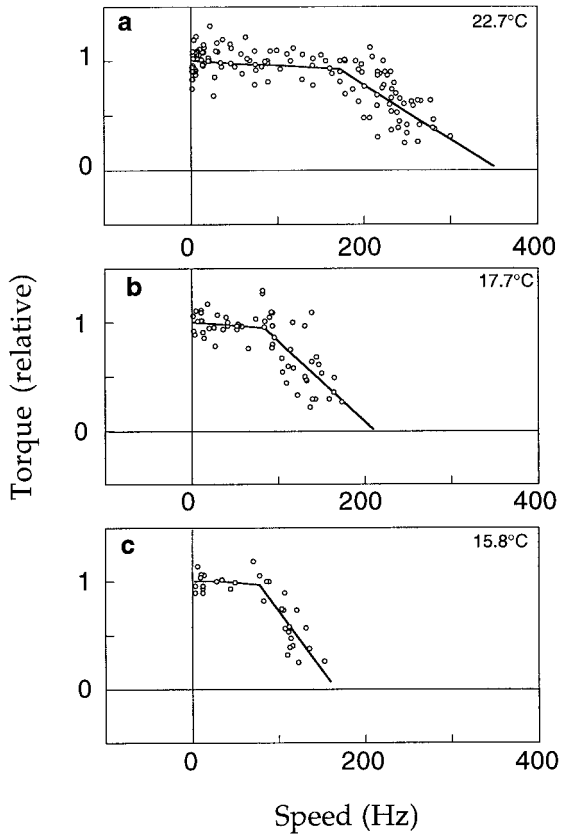

FIGURE 5 Torque-speed data for (*a*) 30 cells at 22.7°C, (*b*) 14 cells at 17.7°C, and (*c*) 11 cells at 15.8°C. Two linear regressions are shown for each panel. Their points of intersection define the "knee speed."

TABLE 1 Bulk viscosities of the Ficoll solutions used in the bead-on-stub experiments

Ficoll conc. (% w/v)	Viscosity (cp) at 22.7°C	17.7°C	15.8°C
0	0.986	1.08	1.14
1	1.16	1.35	1.39
2	1.37	1.60	1.63
3	1.63	1.82	1.95
4	1.93		
5	2.33	2.86	2.90
6	2.73		
7	3.22		
8	3.86	4.44	4.70
9	4.47		
10	5.29	6.33	6.52
12	7.09		8.59
13	8.18		
15	10.84	13.36	13.88

DISCUSSION

We have found, in agreement with earlier work (Berg and Turner, 1993; Berry and Berg, 1999), that torque remains approximately constant up to a relatively high speed (to a knee speed of ~170 Hz at 23°C) and then drops rapidly (to a zero-torque speed of ~350 Hz at 23°C) (Figs. 5 and 7). In the low-speed regime, torque is independent of temperature (Fig. 6). This independence was shown more rigorously for *Streptococcus* (Khan and Berg, 1983). At low speeds, the motor appears to operate near thermodynamic equilibrium, where rates of displacement of internal mechanical components or translocation of protons are not limiting. The transition between the low-speed and high-speed regimes (the knee) shifts to lower speeds at lower temperatures, and the

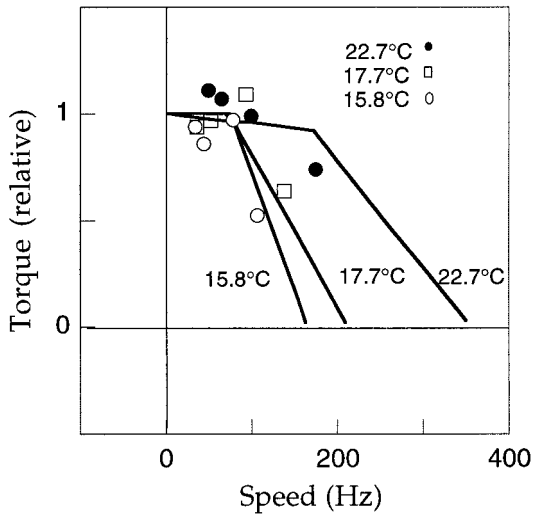

FIGURE 6 Torque-speed data obtained from a single cell at 22.7, 17.7, and 15.8°C. The regression lines of Fig. 5 are included to guide the eye. The Ficoll solutions used were 0, 5, 8, and 10% (for the data points at each temperature, *reading from right to left*).

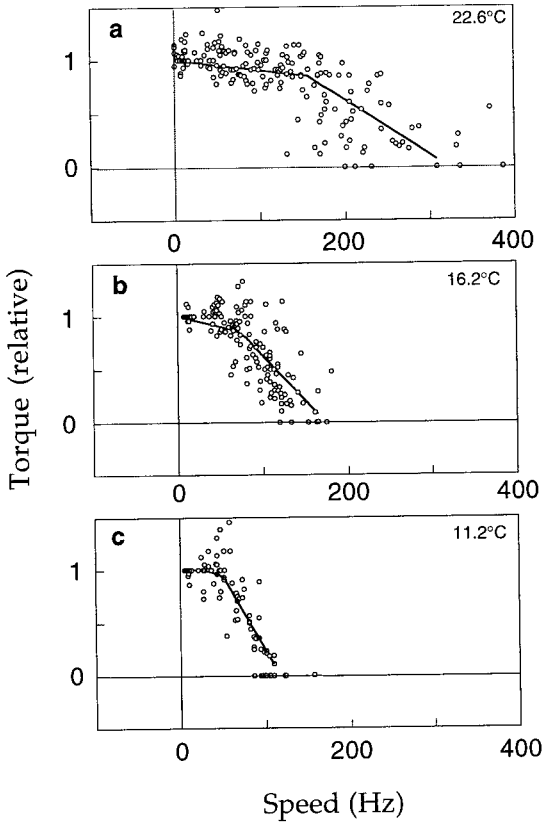

FIGURE 7 Torque-speed data obtained by electrorotation (Berg and Turner, 1993), plotted in the manner of Fig. 5. (*a*) Twenty-seven cells at 22.6°C; (*b*) 33 cells at 16.2°C; (*c*) 17 cells at 11.2°C. Two linear regressions are shown for each panel (determined in the same manner as those in Fig. 5).

rate of decline of torque with speed steepens. Evidently, the rate-limiting step or steps responsible for this loss of torque are strongly temperature dependent. In the high-speed regime, it is known that shifts from H_2O to D_2O also reduce torque (Meister and Berg, 1987; Blair and Berg, 1990), so the rate-limiting step probably involves proton transfer. The knee and zero-torque speeds show a Q_{10} (fractional increase in rate for a temperature increment of 10°C) of ~3 (Table 2). An Arrhenius plot of zero-torque speeds yields a straight line with a slope corresponding to an activation enthalpy of ~18 kcal/mol (not shown). This is too large for a rate-limiting step involving the dissociation of a proton from Asp-32 of MotB (Edsall and Wyman, 1958), an amino acid located near the cytoplasmic end of the putative membrane channel, shown to be critical for proton transfer by Zhou et al. (1998). However, it is similar to the temperature dependence found for other proton channels by DeCoursey and Cherney (1998).

The motor is driven by a proton flux. Only one experiment has attempted to measure this flux (for *Streptococcus*; Meister and Berg, 1987), and flux and speed were found to be linearly related (for speeds up to 65 Hz). Unless protons flow through the motor when it is stalled, this implies that a fixed number of protons carries the motor through each revolution. At low speeds, the running torque is close to the stall torque. If the motor is stalled and no protons flow, then no free energy is dissipated. Therefore, the stalled motor is at thermodynamic equilibrium. For slow rotation near stall, the motor must operate reversibly at unit efficiency, with the free energy dissipated by protons traversing the motor equal to the mechanical work that it performs (Meister and Berg, 1987). This implies that the torque near stall should be proportional to protonmotive force over the latter's full physiological range. This was found to be the case by Fung and Berg (1995) for potentials up to 150 mV and speeds up to 7 Hz. So the evidence supports a model in which the motor is tightly coupled.

If tight coupling persists over the full dynamic range, then the efficiency of the motor remains high up to the knee and then rapidly declines. Beyond the knee, the power output (torque × speed) falls, but the power input (proton flux × charge × protonmotive force) continues to rise. One sce-

TABLE 2 Comparison of results obtained in the present study (Fig. 5) with those obtained by electrorotation (Fig. 7)

Temperature (°C)	Knee speed (Hz)	Relative torque at knee	Zero-torque speed (Hz)
Present study			
22.7	175	0.92	350
17.7	83	0.95	210
15.8	80	1.0	180
Electrorotation			
22.6	156	0.85	322
16.2	70	0.87	173
11.2	50	0.95	117

nario in which this might happen would be if the energy available from proton translocation is used to stretch a spring, which then applies a steady force at the periphery of the rotor. If stretch is generated by a proton-driven conformational change of fixed magnitude, *d*, the work done on the spring will be *Fd*, where *F* is spring tension. When such a system operates near equilibrium, all of this energy is delivered to the rotor, generating a displacement at its periphery, *d*. However, if the rotor is moving so rapidly that displacement of this magnitude occurs before the next proton-driven transformation, the spring will relax, and the tension, *F*, will decline. Hence, when the next conformational change does occur, the work done on the spring will be smaller, and some of the available energy will be dissipated as heat. At the zero-torque speed, the spring will be completely relaxed, and all of the energy will be dissipated as heat. A mechanism of this kind could generate the requisite torque-speed behavior if the energy given up by the proton is transferred to the spring in a single step, that is, if proton translocation and conformational change are directly coupled (Berry and Berg, 1999). This is not expected if proton translocation primes a ratchet that waits for thermal fluctuations to stretch the spring, a mechanism proposed earlier (Berg and Khan, 1983; Khan and Berg, 1983; Meister et al., 1989).

For concise surveys of existing models for the flagellar motor, see Läuger and Kleutsch (1990), Berg and Turner (1993), and Caplan and Kara-Ivanov (1993). For more recent work, see Elston and Oster (1997). Some of these models make explicit predictions for the torque-speed curve. However, most of these models were crafted in the belief that torque drops approximately linearly from stall to the zero-torque speed. This was an historical accident. The first measurements of torque speed made in the high-speed regime were for swimming cells of *Streptococcus*, which ran their motors more slowly in solutions of Ficoll (Lowe et al., 1987). These data could be extrapolated back to points obtained at much lower speeds with tethered cells. However, the uncertainty in the viscous drag on the latter was large, and the linear extrapolation was not valid. Given the measurements described in the present work, some of these models should be revisited.

The methods used in this study were pioneered by Karen Fahrner, who constructed the smooth-swimming sticky-filament strain and prepared the Ficoll stocks, and Richard Berry, who built the optical trap and, with Will Ryu, perfected the bead assay. Linda Turner conducted the electron microscopy.

This work was supported by grant AI16478 from the National Institutes of Health and by the Rowland Institute for Science.

REFERENCES

Berg, H. C. 1993. Random Walks in Biology. Princeton University Press, Princeton, NJ.

Berg, H. C., and S. M. Block. 1984. A miniature flow cell designed for rapid exchange of media under high-power microscope objectives. *J. Gen. Microbiol.* 130:2915–2920.

Berg, H. C., and S. Khan. 1983. A model for the flagellar rotary motor. *In* Mobility and Recognition in Cell Biology. H. Sund and C. Veeger, editors. deGruyter, Berlin. 485–497.

Berg, H. C., and L. Turner. 1993. Torque generated by the flagellar motor of *Escherichia coli. Biophys. J.* 65:2201–2216.

Berry, R. M., and J. P. Armitage. 1999. The bacterial flagellar motor. *Adv. Microb. Physiol.* 41:291–337.

Berry, R. M., and H. C. Berg. 1997. Absence of a barrier to backwards rotation of the bacterial flagellar motor demonstrated with optical tweezers. *Proc. Natl. Acad. Sci. USA.* 94:14433–14437.

Berry, R. M., and H. C. Berg. 1999. Torque generated by the flagellar motor of *Escherichia coli* while driven backwards. *Biophys. J.* 76: 580–587.

Blair, D. F., and H. C. Berg. 1990. The MotA protein of *Escherichia coli* is a proton-conducting component of the flagellar motor. *Cell.* 60: 439–449.

Caplan, S. R., and M. Kara-Ivanov. 1993. The bacterial flagellar motor. *Int. Rev. Cytol.* 147:97–164.

Chen, X. 1999. Dynamic properties of the bacterial flagellar motor of *E. coli.* Ph.D. thesis. Harvard University, Cambridge, MA.

DeCoursey, T. E., and V. V. Cherney. 1998. Temperature dependence of voltage-gated H^+ currents in human neutrophils, rat alveolar epithelial cells, and mammalian phagocytes. *J. Gen. Physiol.* 112:503–522.

Edsall, J. T., and J. Wyman. 1958. Biophysical Chemistry. Academic Press, New York. 450–453.

Elston, T. C., and G. Oster. 1997. Protein turbines. I. The bacterial flagellar motor. *Biophys. J.* 73:703–721.

Fahrner, K. A. 1995. Studies of bacterial flagellar motors and filaments. Ph.D. thesis. Harvard University, Cambridge, MA.

Fung, D. C., and H. C. Berg. 1995. Powering the flagellar motor of *Escherichia coli* with an external voltage source. *Nature.* 375:809–812.

Happel, J., and H. Brenner. 1983. Low Reynolds Number Hydrodynamics. Martinus Nijhoff, The Hague, the Netherlands.

Khan, S., and H. C. Berg. 1983. Isotope and thermal effects in chemiosmotic coupling to the flagellar motor of *Streptococcus. Cell.* 32: 913–919.

Läuger, P., and B. Kleutsch. 1990. Microscopic models of the bacterial flagellar motor. *Comments Theor. Biol.* 2:99–123.

Lowe, G., M. Meister, and H. C. Berg. 1987. Rapid rotation of flagellar bundles in swimming bacteria. *Nature.* 325:637–640.

Macnab, R. M. 1996. Flagella and motility. *In Escherichia coli* and *Salmonella*: Cellular and Molecular Biology. F. C. Neidhardt, R. Curtiss, J. L. Ingraham, E. C. C. Lin, K. B. Low, B. Magasanik, W. S. Reznikoff, M. Riley, M. Schaechter, and H. E. Umbarger, editors. American Society for Microbiology, Washington, DC. 123–145.

Macnab, R., and D. E. Koshland, Jr. 1974. Bacterial motility and chemotaxis: light-induced tumbling response and visualization of individual flagella. *J. Mol. Biol.* 84:399–406.

Meister, M., and H. C. Berg. 1987. The stall torque of the bacterial flagellar motor. *Biophys. J.* 52:413–419.

Meister, M., S. R. Caplan, and H. C. Berg. 1989. Dynamics of a tightly coupled mechanism for flagellar rotation. *Biophys. J.* 55:905–914.

Perrin, J. 1923. Atoms. Constable, London.

Washizu, M., Y. Kurahashi, H. Iochi, O. Kurosawa, S.-I. Aizawa, S. Kudo, Y. Magariyama, and H. Hotani. 1993. Dielectrophoretic measurement of bacterial motor characteristics. *IEEE Trans. Ind. Appl.* 29:286–294.

Zhou, J., L. L. Sharp, H. L. Tang, S. A. Lloyd, S. Billings, T. F. Braun, and D. F. Blair. 1998. Function of protonatable residues in the flagellar motor of *Escherichia coli*: a critical role for Asp 32 of MotB. *J. Bacteriol.* 180:2729–2735.